JPE 11-1-10

Improved Deadbeat Current Controller with a Repetitive-Control-Based Observer for PWM Rectifiers

Jilei Gao†, Trillion Q. Zheng*, and Fei Lin*

†* School of Electrical Engineering, Beijing Jiaotong University, Beijing, China

Abstract

The stability of PWM rectifiers with a deadbeat current controller is seriously influenced by computation time delays and low-pass filters inserted into the current-sampling circuit. Predictive current control is often adopted to solve this problem. However, grid current predictive precision is affected by many factors such as grid voltage estimated errors, plant model mismatches, dead time and so on. In addition, the predictive current error aggravates the grid current distortion. To improve the grid current predictive precision, an improved deadbeat current controller with a repetitive-control-based observer to predict the grid current is proposed in this paper. The design principle of the proposed observer is given and its stability is discussed. The predictive performance of the observer is also analyzed in the frequency domain. It is shown that the grid predictive error can be decreased with the proposed method in the related bode diagrams. Experimental results show that the proposed method can minimize the current predictive error, improve the current loop robustness and reduce the grid current THD of PWM rectifiers.

Key Words: Deadbeat current control, PWM rectifiers, Repetitive control, Time delay

I. Introduction

When compared with conventional diode rectifiers and phase-controlled rectifiers, PWM rectifiers have the advantages of low current harmonic distortions, a high input power factor and the ability to have a bi-directional power flow. For these reasons, PWM rectifiers have been playing important roles as active front end rectifiers in the fields of adjustable speed drives, grid-connected converters for renewable energy systems, and power conditioning and transmission equipment. As the grid side converters of main traction systems and onboard power supply systems, they have been widely used in modern ac drive electric locomotives [1]–[3].

Various control strategies for PWM rectifiers have been proposed to regulate the dc link voltage while improving the quality of the input ac current. A double closed-loop control method is often adopted where the outer loop is a dc voltage loop and the inner loop is a current loop. When using this method the system performance is largely determined by the inner current loop. The hysteresis current control scheme features a fast response, excellent accuracy and easy implementation. However, the variable switching frequency imposes excessive difficulty in designing the main circuit of the converters [4], [5]. The ramp comparison control using a PI regulator has the disadvantage of a steady state phase error between the reference current and the actual current. The PI parameters tuning are also required to suit the load conditions [6]. It is widely known that the steady-state ac error limitation of the ramp comparison control was overcome by "the synchronous frame current control method" proposed by Schauder and Caddy and refined by Rowan and Kerkman [7], [8]. Proportional-resonant current control can also realize a zero steady-state ac error by utilizing its characteristic of infinite gain at the grid frequency but without a rotating frame transformation. However, the poles assignment should be made to obtain a high performance and the tuning process is not straightforward. The performance also largely depends on the microprocessor capability and the discrete method of the resonant controller [9]–[11].

A deadbeat current control algorithm calculates the converter duty cycle according to a plant discrete model in every sampling interval to make sure the grid current tracks the reference in the next interval. It can be easily implemented on digital processors, and it has the excellent characteristic of a fast current response. However, the inherent sampling and computation time delay of digital control and a low-pass filter in the current sample circuit degrades the performance of the converters and reduces its robustness [12]. An ac filtering inductor parameter must be obtained exactly in the controller; otherwise the mismatch will influence the stability. The sampling point should be set just ahead of the controlling point by the period of the total delay to reduce its effects [13], [14]. However, the delay has to be measured accurately.

Manuscript received Sep. 28, 2009; revised Nov. 14, 2010
† Corresponding Author: 06117304@bjtu.edu.cn
Tel: +86-010-5168-4051, Fax: +86-010-5168-4029, Beijing Jiaotong Univ.
* School of Electrical Eng., Beijing Jiaotong University, China

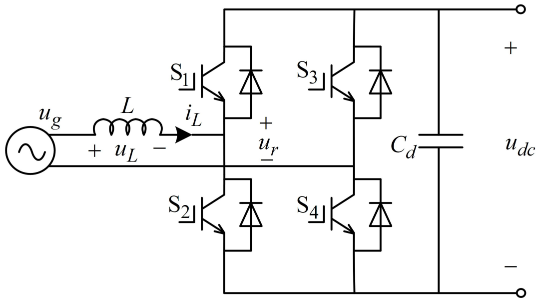

Fig. 1. Power circuit of single-phase PWM rectifiers.

A predictive current controller is often adopted to compensate for the time delay [15], [16]. However, the one-step predictive current method is essentially an open-loop current observer and the prediction error is not converged as in [16]. The current predictive value is influenced by factors such as plant uncertainty, grid voltage estimated error, dead-time, etc. The use of a closed loop predictive observer for predictive deadbeat control is discussed in [17]. Also, an adaptive self-tuning load model was used in a predictive current controller to ensure converter stability and robustness [18], [19].

Recently, a repetitive control (RC), based on the internal model principle, has been successfully applied in the fields of UPS, active power filters, inverters and so on [20]–[25]. RC is an effective method to exactly track periodic reference signals and to eliminate periodic errors.

In this paper, an improved deadbeat current control method with a repetitive-control-based observer is proposed, which can significantly improve the grid current predictive precision in the presence of uncertainties and disturbances. In section II, the current stability of conventional deadbeat control for PWM rectifiers is analyzed considering a one sampling-period delay and a current sample filter. The shortcomings of the open-loop current observer used to compensate the delay are also analyzed in section II. Further, in section III the new observer based on repetitive control is proposed and the design method is given. In section IV, experiments are made to validate the proposed method and comparisons are given between the open-loop predictive current method and the proposed method. The experimental results show that the proposed method is correct and effective.

II. Performance Analysis of Deadbeat Current Control

A. Discrete model of PWM Rectifiers

Fig.1 shows the power circuit of a single-phase PWM rectifier. In this figure, S_1–S_4 represent the power semiconductor devices; u_g and u_r are the grid side and the converter side voltage respectively; L is the ac side filtering inductor; u_L and i_L represent the voltage and the current of the filtering inductor respectively; C_d is the dc link capacitor and u_{dc} is the dc link output voltage.

Assuming the PWM rectifier switching period is a constant value T_s, in the switching period $[kT_s,\ (k+1)T_s]$, the discrete model of the PWM rectifier current-loop plant can be written

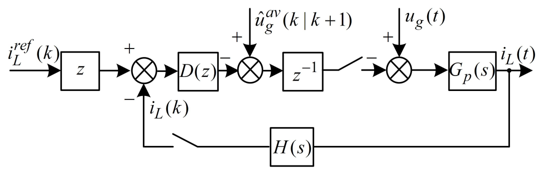

Fig. 2. Control block diagram of the current-loop.

as [5], [12], [13]:

$$u_r^{av}(k|k+1) = u_g^{av}(k|k+1) - \frac{L}{T_s}[i_L(k+1) - i_L(k)] \tag{1}$$

where, ${u_r}^{av}(k|k+1)$ and ${u_g}^{av}(k|k+1)$ denote the average value of the converter side voltage and the grid side voltage over the switching period $[kT_s,\ (k+1)T_s]$, respectively. $i_L(k)$ and $i_L(k+1)$ denote the instantaneous value of the grid current at the sampling points kT_s and $(k+1)T_s$, respectively.

The aim of a current controller is to make the inductor current at the sampling point $(k+1)T_s$ equal to the reference current value ${i_L}^{ref}(k+1)$ at the end of the switching period$[kT_s,(k+1)T_s]$. Therefore the converter side reference voltage in this period can be written as shown in (2) according to the basic principle of the conventional deadbeat current control strategy [16].

$$u_r^{ref}(k) = \hat{u}_g^{av}(k|k+1) - \frac{L}{T_s}\cdot[i_L^{ref}(k+1) - i_L(k)] \tag{2}$$

where, $\hat{u}_g^{av}(k|k+1)$ denotes the average value of the grid voltage in the period $[kT_s,(k+1)T_s]$ and it can be estimated from the previously measured values using linear extrapolation.

B. Stability analysis with the conventional deadbeat current control method

A delay always exists between the sampling of the inductor current and the generation of the converter side voltage, because time for data conversions by the A/D converters and calculations by the microprocessors is required. For the sake of simplicity, one sampling-period delay is assumed to analyze the problem. A discrete control block diagram of a single-phase PWM rectifier is shown in Fig.2.

The delay of one sampling-period is modeled by the z^{-1} block. The ZOH equivalence transfer function of the plant is shown in (3) [12].

$$G_p(z) = (1-z^{-1})\cdot Z[\frac{G_p(s)}{s}] = \frac{T_s}{L}\cdot\frac{1}{z-1}. \tag{3}$$

The deadbeat controller $D(z)$ of the current-loop can be written as:

$$D(z) = \frac{\hat{L}}{T_s} = k_L\frac{L}{T_s} \tag{4}$$

where, $\hat{L}$ is the ac filtering inductance used in the controller and $k_L = \hat{L}/L$ is defined to denote the difference between the inductance used in the controller and the actual value.

A transfer functions of the current-loop without considering the sampling-period delay and with a one sampling-period delay can be described by (5) and (6), respectively.

$$G_1(z) = \frac{z\cdot D(z)\cdot G_p(z)}{1+D(z)\cdot G_p(z)} \tag{5}$$

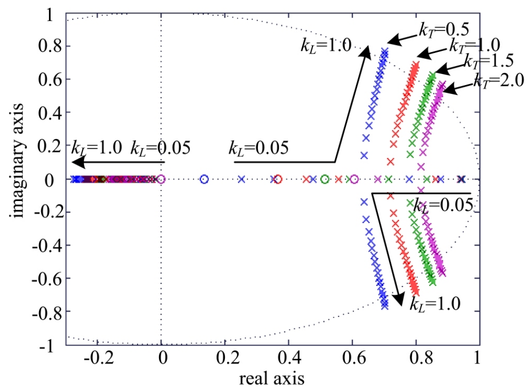

Fig. 3. Root locus of current-loop gain with one sampling-period delay in case of different k_T values.

$$G_2(z) = \frac{D(z) \cdot G_p(z)}{1 + D(z) \cdot z^{-1} \cdot G_p(z)}. \tag{6}$$

Submitting (3) and (4) into (5) and (6), the stability condition of the current loop obtained is $0 < k_L < 2$ and $0 < k_L < 1$ without considering the delay and with a one sampling-period delay, respectively. It can be seen that the robustness for inductance mismatch of the current loop is reduced because of the existence of the delay.

A low-pass filter is often adopted to suppress the influence of switching noises in a current sampling circuit. The filtering transfer function $H(s)$ can be written as (7) assuming that the filtering time coefficient is T_f.

$$H(s) = \frac{1}{T_f s + 1}. \tag{7}$$

Defining the time coefficient $k_T = T_f/T_s$, the discrete transfer function of the plant and the low-pass filter using ZOH can be written as:

$$GH(z) = \frac{T_s}{L} \cdot (-k_T + \frac{1}{z-1} + k_T \cdot \frac{z-1}{z - e^{-\frac{1}{k_T}}}). \tag{8}$$

The current closed-loop transfer function can be described by (9).

$$G_3(z) = \frac{D(z) \cdot G_p(z)}{1 + D(z) \cdot z^{-1} \cdot GH(z)}. \tag{9}$$

Root locus diagrams of a current-loop with a one sampling-period delay in the cases of $k_T = 0.5, 1, 1.5$ and 2 respectively are shown in Fig.3. It is shown that the stability region of k_L is decreased further because of the current sampling filter.

C. Shortcomings of deadbeat control with an open-loop current observer

In order to eliminate the effect of a one sampling-period delay, a modified deadbeat current control method with an open-loop current observer, which is called predictive current control in the literatures was proposed as shown in (10). A timing schematic of a deadbeat controller with an open-loop current observer is shown in Fig.4. The sampling point is set on the instant when the DSP timer counter register value becomes zero to eliminate the switching noises [5].

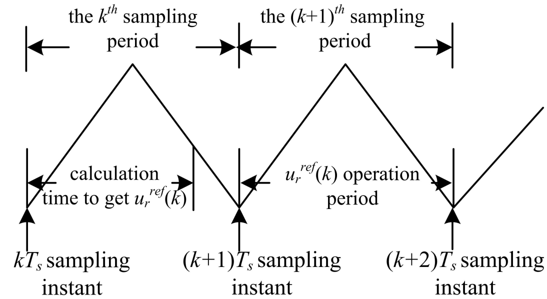

Fig. 4. Timing schematic of deadbeat current controller with open-loop current observer.

$$u_r^{ref}(k) = \hat{u}_g^{av}(k+1|k+2) - \frac{\hat{L}}{T_s} \cdot [i_L^{ref}(k+2) - \hat{i}_L(k+1)] \tag{10}$$

where, the grid current $\hat{i}_L(k+1)$ at $(k+1)T_s$ instant can be predicted according to (11):

$$\hat{i}_L(k+1) = \frac{T_s}{\hat{L}} \cdot [\hat{u}_g^{av}(k|k+1) - u_r^{ref}(k-1)] + i_L(k) \tag{11}$$

while the actual grid current at $(k+1)T_s$ instant can be described as,

$$i_L(k+1) = \frac{T_s}{L} \cdot [u_g^{av}(k|k+1) - u_r^{av}(k|k+1)] + i_L(k). \tag{12}$$

By comparing (11) and (12), it can be concluded that the predictive current value is influenced by the grid voltage estimated error, the plant model mismatch and the dead-time, etc. Assuming $\Delta u(k|k+1)$ represents the equivalent voltage error caused by the factors mentioned above, the predictive current error $e(k+1)$ at the $(k+1)$ T_s instant can be written as:

$$e(k+1) = \frac{T_s}{L} \Delta u(k|k+1). \tag{13}$$

The actual grid current value at $(k+2)T_s$ instant can be described as:

$$i_L(k+2) = \frac{T_s}{L} \cdot [u_g^{av}(k+1|k+2) - u_r^{av}(k+1|k+2)] + i_L(k+1). \tag{14}$$

According to (10) and (14), the grid current tracking error $\Delta i(k+2)$ at $(k+2)T_s$ instant can be expressed as:

$$\Delta i(k+2) = e(k+1) + e(k+2). \tag{15}$$

From (15), it is known that the predictive current error will increasingly distort the grid current and increase the low-order current harmonics proportion. Therefore, improving the predictive current precision is an effective method to minimize the grid current harmonics with a predictive current controller.

III. Improved Deadbeat Current Control Method with the Proposed Observer

A. Proposed repetitive-control-based observer

From the analysis in section II, it is shown that the predictive current value is seriously affected by the grid voltage extrapolation error, the dead-time and the plant model mismatch. It is worth emphasizing that all of these disturbances are periodic signals at the grid voltage frequency. It is well known

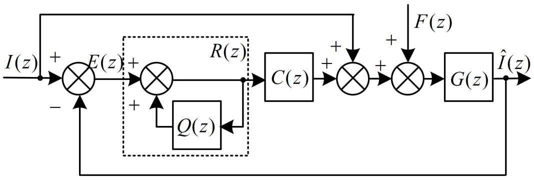

Fig. 5. Block diagram of repetitive-control-based observer.

that repetitive control based on the internal mode principle is an effective control method to eliminate periodic external disturbances. A closed-loop current observer using repetitive control is proposed in this section to improve the predictive current precision.

A control diagram of the proposed observer is shown in Fig.5. The basic repetitive controller can be written as:

$$R(z) = \frac{1}{1-Q(z)} = \frac{1}{1-k_q z^{-N}} \tag{16}$$

where, k_q is usually a low-pass zero-phase filter or a constant smaller than 1 to ensure that the observer is stable. It results in a tradeoff between tracking accuracy and system robustness [21]. For simplicity of analysis, it is chosen as a constant 0.98 here. N is the sampling times in a grid fundamental period.

The transfer function $C(z)$ in Fig. 5 aims to compensate the frequency characteristics of the observer plant $G(z)$ which is the one sampling-period delay shown in (17):

$$G(z) = z^{-1}. \tag{17}$$

Therefore the compensator $C(z)$ is chosen as $k_r z^{N+1}$ which has the characteristics of a one sampling-period lead to compensate for the delay of the plant. k_r is the loop gain of the grid current observer. Then, the current observer can be obtained as shown in (18) according to Fig.5.

$$\hat{I}(z) = I(z)G(z) + F(z)G(z) + R(z)C(z)G(z)E(z) \tag{18}$$

where, $I(z)$ and $F(z)$ are the feed forward compensators which are the same as the expression shown in (11) with the open-loop predictive current method.

$$E(z) = I(z) - \hat{I}(z). \tag{19}$$

Without considering $F(z)$, the closed-loop transfer function of the observer $G_o(z)$ can be written as,

$$G_o(z) = \frac{G(z) + R(z)C(z)G(z)}{1 + R(z)C(z)G(z)}. \tag{20}$$

The observer stability condition is that the roots of the characteristic polynomial of the closed-loop transfer function, $1 + R(z)C(z)G(z)$, are inside the unit circle. The stability condition can be calculated as,

$$0 < k_r < 1.98. \tag{21}$$

However, the condition shown in (21) can just ensure that the current observer is stable. To guarantee that the whole current loop is stable, the value of k_r must be much smaller than 1.98 as shown in (21). Here k_r is chosen as 0.1. A Bode diagram of the proposed current observer closed-loop transfer function is plotted in Fig.6 when k_r is equal to 0.1. It presents

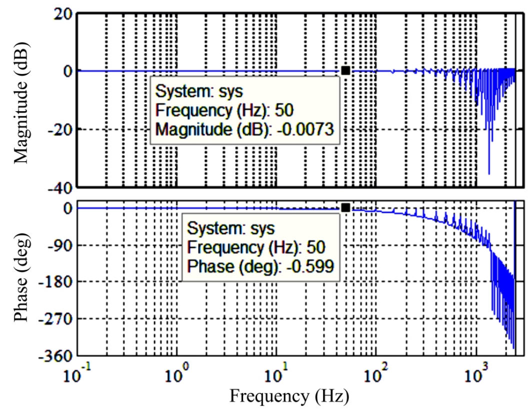

Fig. 6. Bode diagram of the proposed observer.

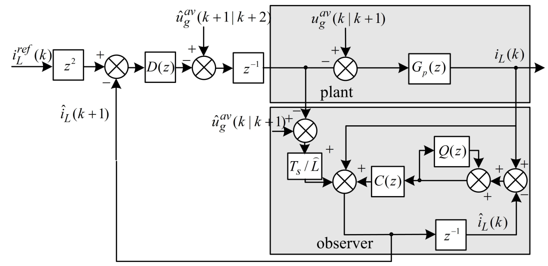

Fig. 7. Control block diagram of improved deadbeat controller with repetitive-control-based observer.

prefect tracking at grid frequency. The current observer can eliminate the disturbance produced by the factors analyzed in the former section. A control block diagram of the improved deadbeat controller with a repetitive-control-based observer is shown in Fig.7.

B. Comparisons with an open-loop current observer

The predictive current value using the proposed observer at the $(k+1)T_s$ instant can be obtained as:

$$\hat{i}_L(k+1) = \frac{T_s}{\hat{L}} \cdot [\hat{u}_g^{av}(k|k+1) - u_r^{ref}(k-1)] + i_L(k) + \frac{k_r z^{-N+1}}{1-k_q z^{-N}}[i_L(k) - \hat{i}_L(k)]. \tag{22}$$

The predictive current error can be written as shown in (23) by subtracting (22) from (12).

$$e(k+1) = \frac{T_s}{L}\Delta u(k|k+1) - \frac{k_r z^{-N+1}}{1-k_q z^{-N}} e(k). \tag{23}$$

The error transfer function which represents the frequency characteristics of the predictive current error $e(k+1)$ versus the equivalent voltage error $\Delta u(k|k+1)$ with the proposed observer based on repetitive control is shown in (24).

$$G_{eclosed}(z) = \frac{T_s}{L} \cdot \frac{1-k_q z^{-N}}{1+(k_r-k_q)z^{-N}}. \tag{24}$$

The error transfer function with an open-loop observer can be concluded by (13) as,

$$G_{eopen}(z) = \frac{T_s}{L}. \tag{25}$$

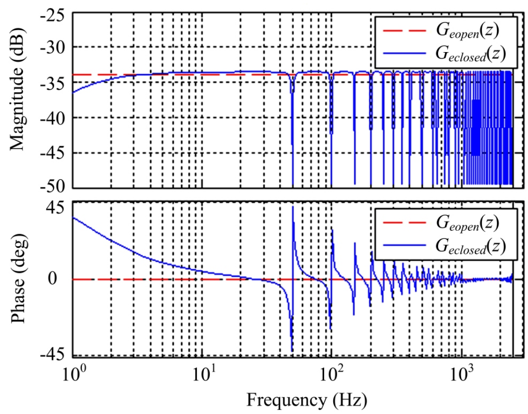

Fig. 8. Bode diagram of the error transfer function with open-loop and the proposed observer.

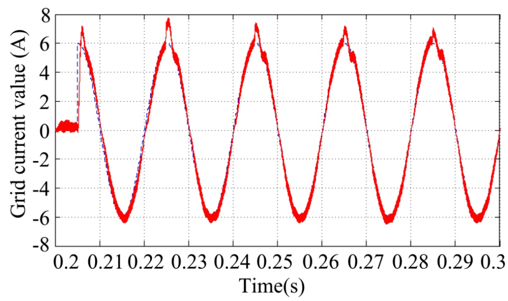

(a)

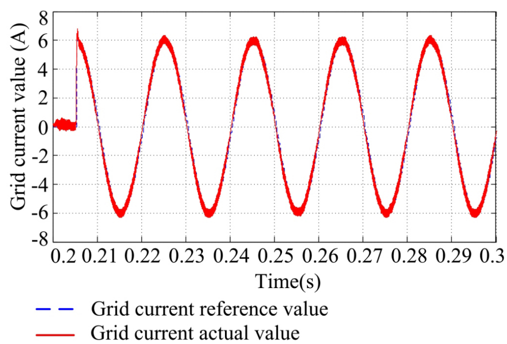

(b)

Fig. 9. Waveforms of grid current reference value and actual value (a) with repetitive current controller combined with deadbeat control (b) with the improved deadbeat control proposed in this paper.

When the switching frequency is 5 kHz and the ac filtering inductance is 10.4mH, the frequency characteristics of the error transfer function of the open-loop and the proposed observer in this paper are shown in Fig.8 with a dash line and a continuous line, respectively. It is obviously that the predictive current error caused by the equivalent voltage error is much smaller with the proposed observer than with the open-loop one at the grid voltage integer times frequency. As a result, the grid current will have lower low-order harmonics with the proposed method.

C. Simulation Comparisons with the current-loop repetitive control

Repetitive control has rejection capability against repetitive disturbances with a known period. However, it has the disadvantage of a slow dynamic response because the input error of the repetitive controller is used to modify the output by delaying N sampling periods as shown in Fig.5. Therefore, repetitive control is often combined with deadbeat control or proportional-integral control to improve its dynamic performance when it is applied directive in the current loop controller. Even so, the dynamic performance is not satisfying when the current reference changes rapidly. The current amplitude reference value may be a step signal in the application of electric drives with a dc current feed forward to improve the dc link voltage dynamic performance and in the application of fictitious loads in the condition of a simulating step suddenly applied load.

The reason for the poor dynamic performance is analyzed following when the repetitive controller is directive applied to the current controller. If the current amplitude reference value step increases at the $(k-N)T_s$ instant, the input current error will become very large. The large error is applied to modify the controller output at the kT_s instant because of the repetitive controller. However, the actual steady-state current error is small under the action of a deadbeat controller or a proportional-integral controller by this time. Therefore, the current error will become large because the large current error at the $(k-N)T_s$ instant is added to the controller output at the kT_s instant by the repetitive controller.

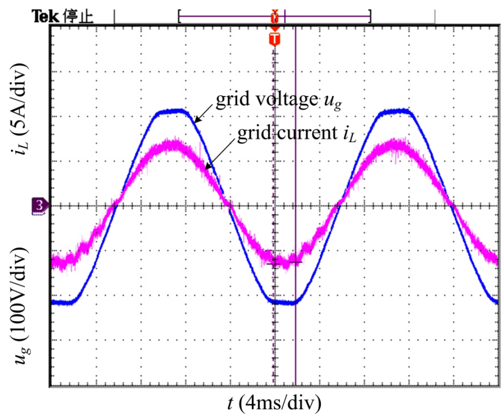

(a)

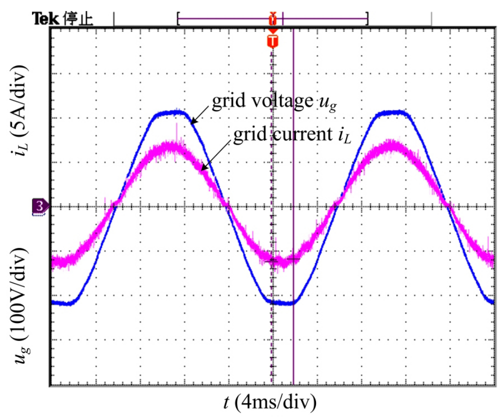

(b)

Fig. 10. Waveforms of grid voltage and current without current observer (*a*) in condition of $k_T = 1$ and $k_L = 1$ (*b*) in condition of $k_T = 1$ and $k_L = 0.95$.

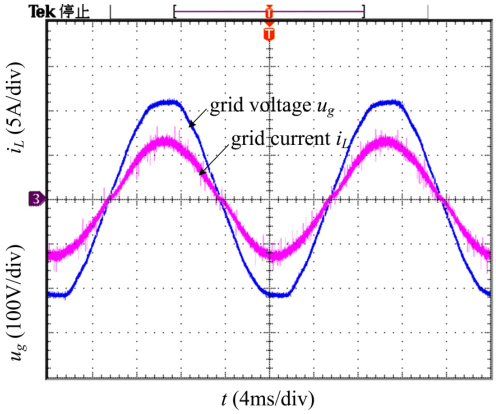

(a)

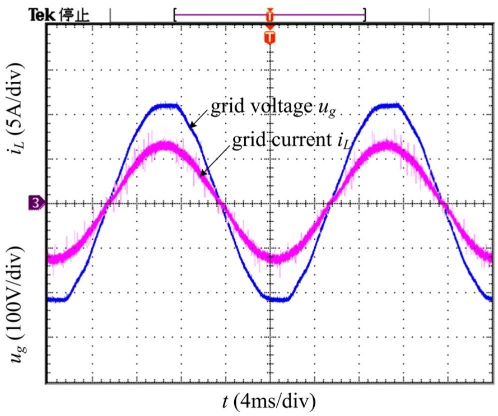

(b)

Fig. 11. Waveforms of grid voltage and current in condition of $k_T = 1$ and $k_L = 1$ (*a*) with open-loop current observer (*b*) with the proposed current observer.

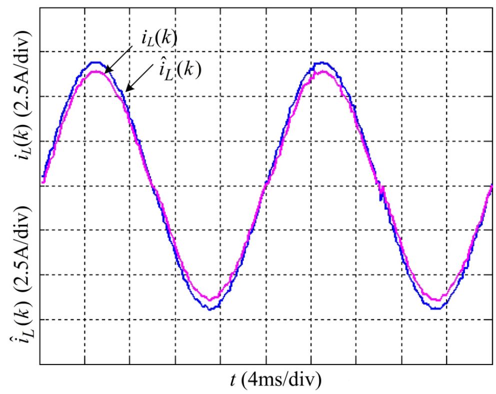

(a)

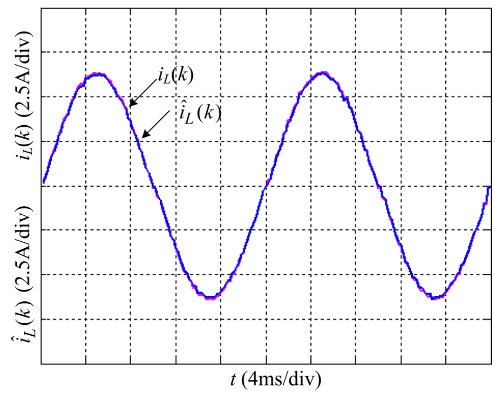

(b)

Fig. 12. Waveforms of actual current and predicted current in condition of $k_T = 1$ and $k_L = 1$ (*a*) with open-loop current observer (*b*) with the proposed current observer.

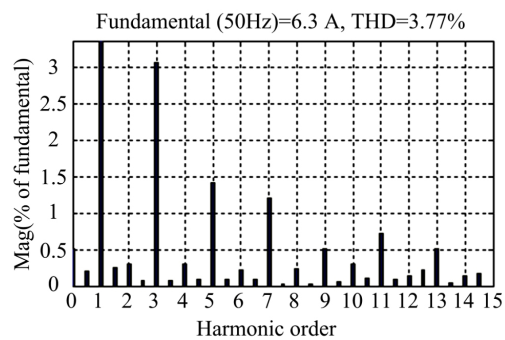

(a)

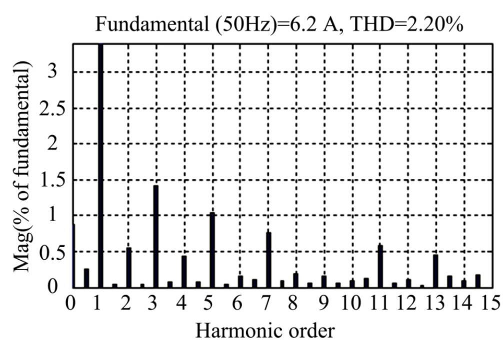

(b)

Fig. 13. Spectrums of grid currents in condition of $k_T = 1$ and $k_L = 1$ (*a*) with open-loop current observer (*b*) with the proposed current observer.

When the repetitive controller is used to predict the grid current, the predictive current error will not become very large because of the feed forward compensator $F(z)$ shown in (18). The current controller is just a deadbeat controller. It has a better dynamic performance but a lower rejection capability against grid voltage harmonic disturbance when compared with a directive repetitive current control.

The simulation results are shown in Fig.9 with the repetitive current controller combined with deadbeat control and with the proposed method in this paper when the current amplitude reference value step increases. It is shown that the grid current amplitude reference step changes at 0.205s, and that there are large overshoots at several fundamental periods after that with a repetitive current controller combined with deadbeat control. However, the grid current can track the reference perfectly using the proposed control method in this paper. It is shown that predictive control with a repetitive-control-based current observer has better dynamic performance than a repetitive current controller combined with deadbeat control.

IV. Experiment Results

In this section, experiment results with the three types of deadbeat current control methods discussed in this paper are presented and comparisons are made to validate the high performance of the proposed method. The main circuit structure

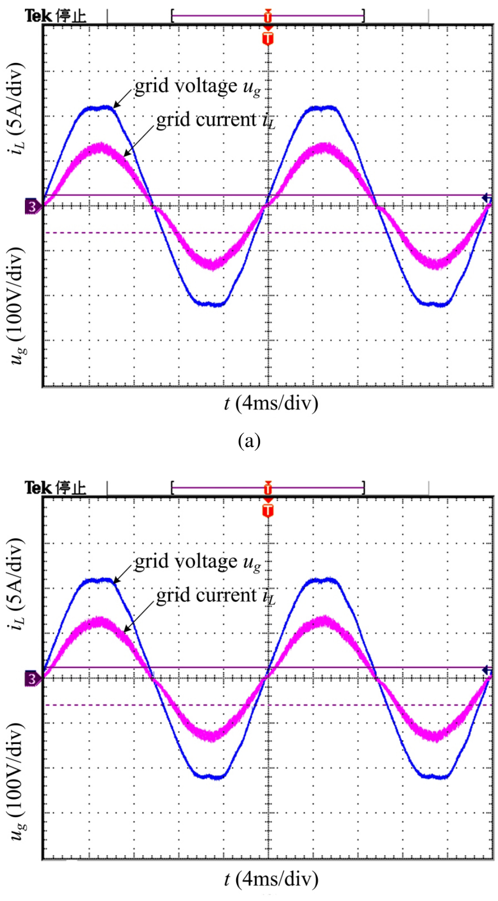

Fig. 14. Waveforms of grid voltage and current in condition of $k_T = 1$ and $k_L = 0.5$ (*a*) with open-loop current observer (*b*) with the proposed current observer.

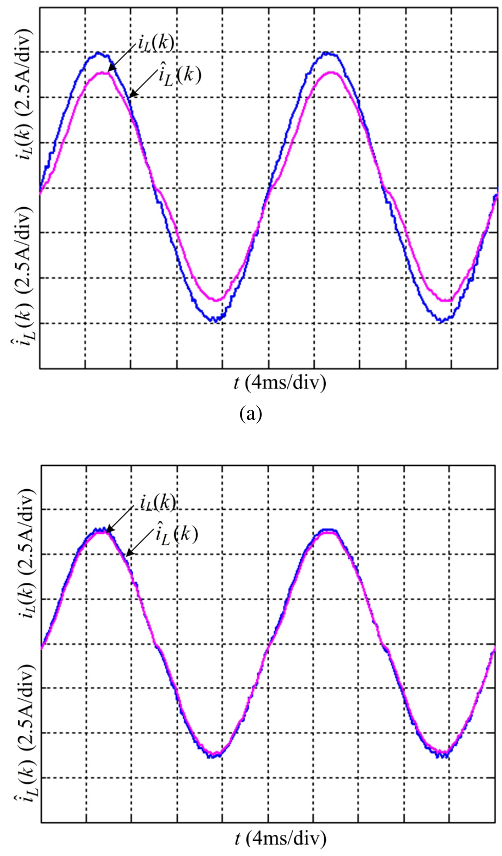

Fig. 15. Waveforms of actual current and predicted current in condition of $k_T = 1$ and $k_L = 0.5$ (*a*) with open-loop current observer (*b*) with the proposed current observer.

TABLE I
SINGLE-PHASE PWM RECTIFIER PARAMETERS

Input voltage(ac)	160 V
Output voltage(dc)	300 V
Filtering inductance	10.4 mH
Dc link Capacitance	470 μF
Load Resistance	140 Ω
Switching Frequency	5 kHz
Dead Time	4 μs

of the experimental setup is the same as the one shown in Fig.1. A power resistor is used as the load of the single-phase PWM rectifier. The control methods are implemented on a TMS320LF2407A produced by TI Company. The experimental parameters of the single-phase PWM rectifiers utilized in this study are listed in Table I.

A. Impact of a current sampling filter on conventional deadbeat control

Fig.10 shows the grid voltage and the current experimental waveforms of a conventional deadbeat current control method without a current observer using the same current sampling filter ($k_T = 1$) but a different k_L value. It is shown that the grid current is unstable in the conditions of both $k_L = 1$ and $k_L = 0.95$. Although k_L is smaller than 1 in Fig.10 (*b*), the current is still unstable because of the current sampling-filter's impact.

B. Comparisons between the two current observer

The grid voltage and the current waveforms with an open-loop current observer and the proposed repetitive-control-based current observer are shown in Fig.11 under the same conditions as in Fig.10. It is shown that the grid currents are stable with both control methods.

To compare the predictive precision of the two observers, the actual current and the predictive current waveforms exported from the DSP debug environment CCS are plotted in Matlab as shown in Fig.12. It is seen that the predictive current error is larger near the peak of the current waveforms in Fig.12 (*a*) with an open-loop current observer than it is in Fig.12 (*b*) with the proposed observer. The predictive current value is in coincidence with the actual current value perfectly in Fig.12 (*b*). It is indicated that the proposed observer can improve the current predictive precision.

The spectrums of the grid currents shown in Fig.11 are illustrated in Fig.13. The magnitude of the odd harmonics is much smaller with the proposed observer than that with an open-loop current observer as shown in Fig.13. The total harmonic distortion factor (THD) is 2.20% in Fig.13 (*b*), while it is 3.77% in Fig.13 (*a*). Therefore, it can be concluded that the grid current harmonics can be reduced by the proposed current observer based on repetitive control.

The experimental results in the condition of $k_T = 1$ and $k_L = 0.5$ are shown in Fig.14-Fig.16. It is shown that the

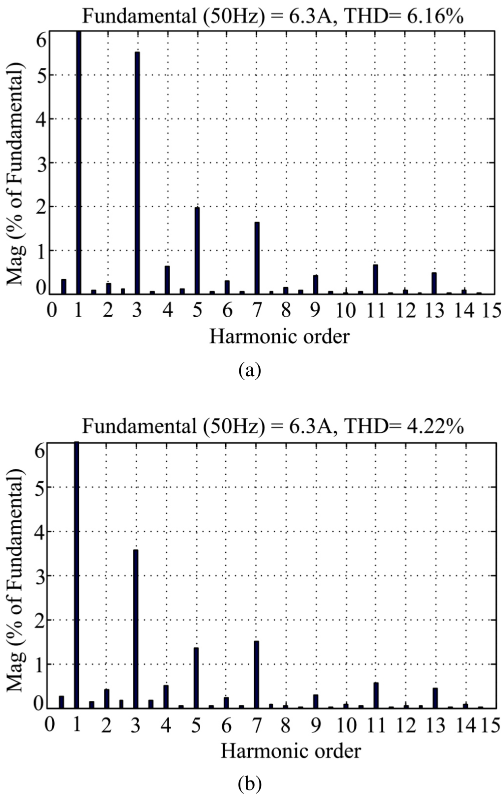

Fig. 16. Spectrums of grid currents in condition of $k_T = 1$ and $k_L = 0.5$ (*a*) with open-loop current observer (*b*) with the proposed current observer.

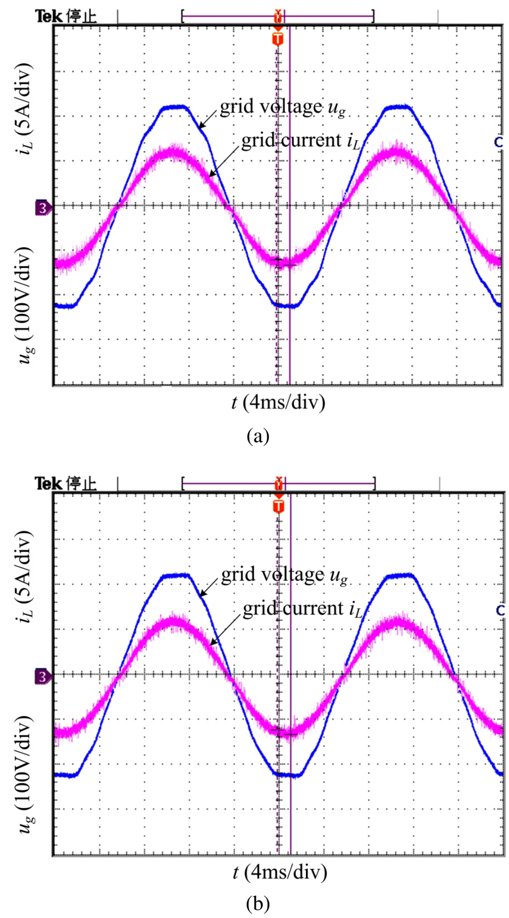

Fig. 17. Waveforms of grid voltage and current in condition of $k_T = 1$ and $k_L = 1.5$ (*a*) with open-loop current observer (*b*) with the proposed current observer.

grid current distortion becomes serious in Fig.14 because the k_L value is too small and the grid current can not track the reference very well. Fig.15 shows the observer response with an open-loop method and the proposed method in this paper. The predictive error becomes much larger in Fig.15 (*a*) than it is in Fig.12 (*a*) due to the small k_L value. However, in Fig.15 (*b*) the predictive current value can still track the actual value with the repetitive-control-based observer very well. It is indicated that the proposed observer has perfect tracking performance although the ac filtering inductance used in the controller is much smaller than its actual value.

Fig.16 gives the grid current spectrums with different current predictive methods in the condition of $k_T = 1$ and $k_L = 0.5$. The total harmonic distortion (THD) of the grid current shown in Fig.14 (*a*) using an open-loop current observer is 6.16%, while it is reduced to 4.22% by the proposed method.

To verify the robustness of a PWM rectifier in case of a plant mismatch, Fig.17 shows the grid voltage and the current waveforms in the condition of $k_T = 1$ and $k_L = 1.5$. The experimental results show that the grid currents are still stable even if k_L is larger than 1. It is shown that the predictive current control method has better robustness than traditional deadbeat control. There is also less current distortion in Fig.17 (*b*) than in Fig.17 (*a*). The proposed predictive current method can eliminate the grid current harmonic caused by a grid current predictive error.

The grid current waveforms with a grid current observer are given in Fig.18 in the condition of $k_T = 1$ and $k_L = 1.5$. It can be seen in Fig.18 that the repetitive-control-based observer still has better predictive performance than an open-loop observer while the larger predictive current error near the peak of the current waveforms still exists in Fig.18 (*a*). Fig.19 presents the spectrums of the grid currents shown in Fig.17. According to the spectrums shown in Fig.19, the current harmonics are decreased by the proposed observer from 2.98% to 1.67%.

V. Conclusions

The performance of a traditional deadbeat current controller was analyzed in this paper. An improved deadbeat current controller with a repetitive-control-based observer has been proposed to improve the grid current predictive precision. The design guidelines have been given to make sure the observer is stable. In addition, the current predictive performance with the proposed observer has been compared with an open-loop observer in the frequency domain. It is shown that the proposed method can decrease the grid current predictive error caused by the equivalent voltage error in the related bode diagrams.

The proposed current observer is applied to a single-phase PWM rectifier to validate the theoretical analysis. The experimental results show that the improved deadbeat current controller with a repetitive-control-based observer can make the rectifiers more robust than a traditional deadbeat current controller. The current predictive precision can be improved in the conditions of both correct and incorrect inductances used

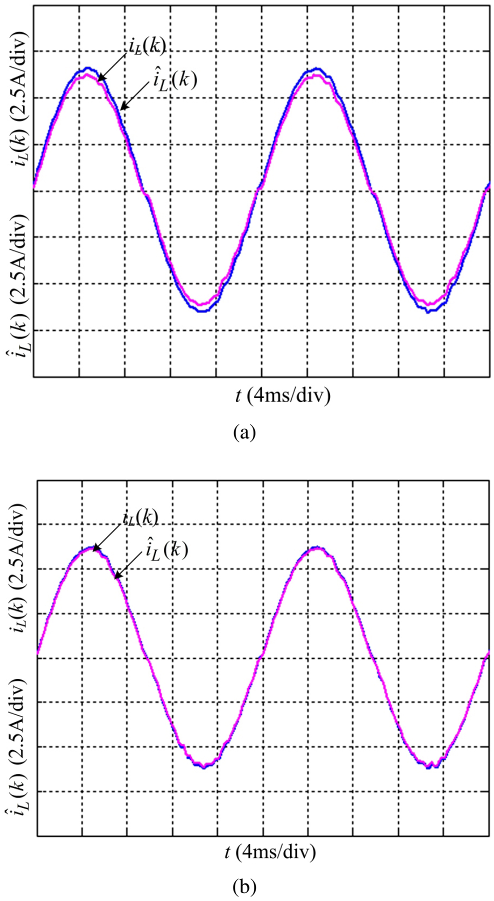

Fig. 18. Waveforms of actual current and predicted current in condition of $k_T = 1$ and $k_L = 1.5$ (*a*) with open-loop current observer (*b*) with the proposed current observer.

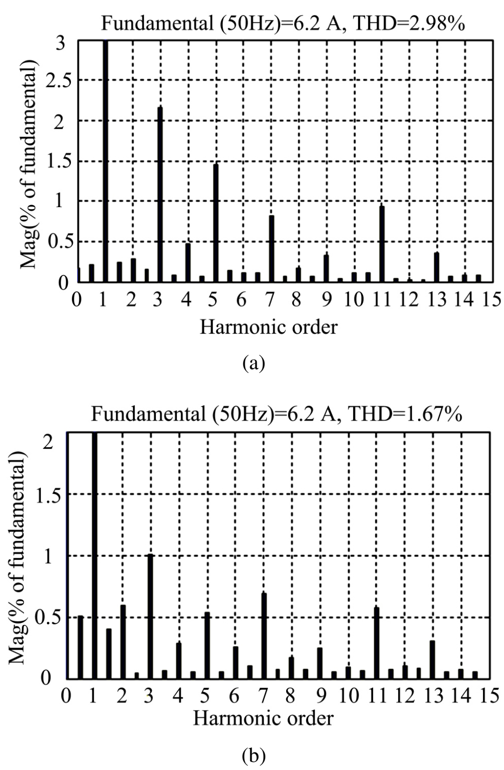

Fig. 19. Spectrums of grid currents in condition of $k_T = 1$ and $k_L = 1.5$ (*a*) with conventional predictive method (*b*) with the proposed method.

in microprocessors. It can be seen that the grid current THD is much lower when using the proposed method in the FFT analysis results.

REFERENCES

[1] G. W. Chang, et. al., “Modeling characteristics of harmonic currents generated by high-speed railway traction drive converters,” *IEEE Transactions on Power Delivery*, Vol. 19, No. 2, pp. 766-773, Apr. 2004.

[2] M. Macan, “Presentation of a four-quadrant converter based system in traction applications-reference to modeling, simulation and analysis,” *European Conference on Power Electronics and Applications,* pp. 1-9, Sep. 2007.

[3] C. Heising, et. al., “Single-phase 50-kw 16.7-Hz four-quadrant line-side converter for railway traction application,” *in Proceeding of EPE-EPMC*, pp. 521-527, Sep. 2008.

[4] O. Kukrer and H. Komurcugil, “Control strategy for single-phase PWM rectifiers,” *Electronics Letters*, Vol. 33, No. 21, pp. 1745-1746, Oct. 1997.

[5] H. Chih-Chiang, et. al., “A digital predictive current control with improved sampled inductor current for cascaded inverters,” *IEEE Transactions on Industrial Electronics*, Vol. 56, No. 5, pp. 1718-1726, May 2009.

[6] R. D. Lorenz and D. B. Lawson, “Performance of feed forward current regulator for field oriented induction machine controllers,” *IEEE Transactions on Industry Applications*, Vol. IA-23, No. 4, pp. 597–602, Jul./Aug. 1987.

[7] C. D. Schauder and R. Caddy, “Current control of voltage source inverters for fast four quadrant drive performance,” *IEEE Transactions on Industry Applications*, Vol. IA-18, No. 2, pp. 163-71, Mar. 1982.

[8] T. M. Rowan and R. J. Kerkman, “A new synchronous current regulator and an analysis of current regulated PWM inverters,” *IEEE Transactions on Industry Applications*, Vol. IA-22, No. 4, pp. 678-690, Jul. 1986.

[9] N. Z. Daniel, et. al., “Stationary frame current regulation of PWM inverters with zero steady-state error,” *IEEE Transactions on Power electronics*, Vol. 18, No. 3, pp. 814-822, May 2003.

[10] L. Pablo, et. al., “Zero-steady-state-error input-current controller for regenerative multilevel converters based on single-phase cells,” *IEEE Transactions on Industrial Electronics*, Vol. 54, No. 2, pp. 733-740, Apr. 2007.

[11] S. Hong-Seok, et. al., “Advanced control scheme for a single-phase PWM rectifier in traction applications,” *in Proceeding of IAS*, Vol.3, pp. 1558-1565. Oct. 2003.

[12] G. K. Hung, et. al., “Analysis and implementation of a delay-compensated deadbeat current controller for solar inverters,” *IEE Proc.-Circuits Devices Syst.*, Vol. 148, No. 5, pp. 279-286, Oct. 2001.

[13] B. Yu, et. al., “Improved predictive current controlled PWM for single-phase grid-connected voltage source inverters,” *in Proceeding of PESC*, pp. 231-236. Jun. 2005.

[14] M. K. Hossein, et. al., “A novel DSP-based current-controlled PWM strategy for single phase grid connected inverters,” *IEEE Transactions on Power Electronics*, Vol. 21, No. 4, pp. 985-993, Jul. 2006.

[15] D. M. Brod and D. W. Novotny, “Current control of VSI-PWM inverters,” *IEEE Transactions on Industry Applications*, Vol. IA-21, No. 4, pp. 562-570, May 1985.

[16] D. G. Holmes and D. A. Martin, “Implementation of a direct digital predictive current controller for single and three phase voltage source inverters”, in *Proceeding of IAS*, Vol. 2, pp. 906-913. San Diego, Oct. 1996.

[17] L. Ben-Brahim and A. Kawamura, “Digital current regulation of field-oriented controlled induction motor based on predictive flux observer,” *IEEE Transactions on Industry Applications*, Vol. 27, No. 5, pp. 956-961, Sep./Oct. 1991.

[18] Y. Abdel-Rady, et. al., “Robust high bandwidth discrete-time predictive current control with predictive internal model-a unified approach for voltage-source PWM converters,” *IEEE Transactions on Power electronics*, Vol. 23, No. 1, pp. 126-136, Jan. 2008.

[19] Y. Abdel-Rady, et. al., “An improved deadbeat current control scheme with a novel adaptive self-tuning load model for a three-phase PWM voltage-source inverter,” *IEEE Transactions on Industrial Electronics*, Vol. 54, No. 2, pp. 747-759, Apr. 2007.

[20] K. L. Zhou and D. W. Wang, “Digital repetitive controlled three-phase PWM rectifier,” *IEEE Transactions on Power Electronics*, Vol. 18, No. 1, pp. 309-316, Jan. 2003.

[21] Y. Q. Ye, et. al., "High-performance repetitive control of PWM DC-AC converters with real-time phase-lead FIR filter," *IEEE Transactions on Circuits and Systems*, Vol. 53, No. 8, pp. 768-772, Aug. 2006.
[22] B. Zhang, et. al., "Linear phase lead compensation repetitive control of a CVCF PWM inverter," *IEEE Transactions on Industrial Electronics*, Vol. 55, No. 4, pp. 1595-1602, Apr. 2008.
[23] X. H. Wu, et. al., "DC link voltage and supply-side current harmonics minimization of three phase PWM boost rectifiers using frequency domain based repetitive current controllers," *IEEE Transactions on Power Electronics*, Vol. 23, No. 4, pp. 1987-1997, Jul. 2008.
[24] R. Costa-Castelló, et. al., "Odd-harmonic digital repetitive control of a single-phase current active filter," *IEEE Transactions on Power Electronics*, Vol. 19, No. 4, pp. 1060-1068, Jul. 2004.
[25] A. García-Cerrada, et. al., "Application of a repetitive controller for a three phase active power filter," *IEEE Transactions on Power Electronics*, Vol. 22, No. 1, pp. 237-246, Jan. 2007.

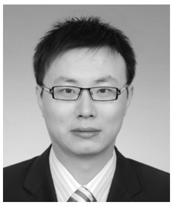

Jilei Gao was born in Shandong Province, China in 1982. He received his B.S. in Electrical Engineering from Beijing Jiaotong University, China, in 2006. Since 2006, he has been a Ph.D. candidate in Electrical Engineering, Beijing Jiaotong University. His research interests focus on the digital control of PWM rectifiers.

Trillion Q. Zheng was born in Zhejiang Province, China in 1964. He received his B.S. from Southwest Jiaotong University, China, in 1986, and his M.S. and Ph.D. from Beijing Jiaotong University, China, in 1992 and 2002, respectively, all majoring in Electrical Engineering. In 1992, he joined Beijing Jiaotong University as an Assistant Professor and he became an Associate Professor in 1997. Since 2000, he has been a Professor in Electrical Engineering. He has served as the Dean of the School of Electrical Engineering at Beijing Jiaotong University since 2003. In 1999, he worked in the Center for Power Electronics at Virginia Polytechnic Institute and State University as a Visiting Professor. His research interests focus on power electronics and motor drives, including converters and drives for EMUs and electric locomotives, wind and PV power generation, power electronics based power quality improvements, etc. Dr. Zheng has published more than 50 journal papers and held 6 patents. He is a senior member of IEEE.

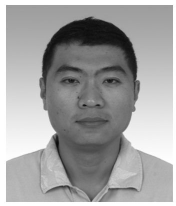

Fei Lin was born in Shandong Province, China in 1975. He received his B.S., M.S. and Ph.D. in Electrical Engineering from Xi'an Jiaotong University, China, Shandong University, China and Tsinghua University, China, in 1997, 2000 and 2004, respectively. Since 2004, he has been with School of Electrical Engineering, Beijing Jiaotong University, where he is currently an Associate Professor. His research interests are in the areas of power electronics and motor control. Dr. Lin is a member of IEEE.